Earth and Planetary Science Letters 593 (2022) 117646

Contents lists available at ScienceDirect

Earth and Planetary Science Letters

www.elsevier.com/locate/epsl

Intracontinental and arc-related hydrothermal systems display distinct δ^{202}Hg and Δ^{199}Hg features: Implication for large-scale mercury recycling and isotopic fractionation in different tectonic settings

Changzhou Deng [a], Bernd Lehmann [b], Tingting Xiao [a], Qinping Tan [a], Di Chen [a,c], Zhendong Tian [a], Xueyun Wang [a,c], Guangyi Sun [d], Runsheng Yin [a,*]

[a] State Key Laboratory of Ore Deposit Geochemistry, Institute of Geochemistry, Chinese Academy of Sciences, Guiyang 550081, China
[b] Mineral Resources, Technical University of Clausthal, Clausthal-Zellerfeld, Germany
[c] University of Chinese Academy of Sciences, Beijing, 100049, China
[d] State Key Laboratory of Environmental Geochemistry, Institute of Geochemistry, Chinese Academy of Sciences, Guiyang 550081, China

ARTICLE INFO

Article history:
Received 1 September 2021
Received in revised form 21 May 2022
Accepted 25 May 2022
Available online 9 June 2022
Editor: L. Coogan

Keywords:
intracontinental hydrothermal systems
mercury isotopes
recycling
isotopic heterogeneity

ABSTRACT

Mercury isotopes display both mass-dependent and mass-independent fractionation and allow the tracing of pathways and storage of surface-derived Hg in the lithosphere. While the subduction-related orogenic recycling of Hg from marine reservoirs into hydrothermal systems in continental arc settings has been documented recently, the source of Hg in intracontinental hydrothermal systems remains unclear. We measured Hg isotopes in two intracontinental anorogenic/postorogenic Late Mesozoic hydrothermal gold deposits in the South China craton and the Central Asian orogenic belt of northern China, respectively. The ore and sulfide samples from the studied systems have positive δ^{202}Hg (0.70 ± 0.39‰, 1SD, n = 49) and negative Δ^{199}Hg values (−0.12 ± 0.05‰, 1SD, n = 49). These values are different from their country rocks and regional geological environment (volcanic arc granites, marine sedimentary rocks) which have positive Δ^{199}Hg values, but similar to that of their Precambrian supracrustal basement rocks of largely non-marine continental materials. We conclude that Hg in the intracontinental hydrothermal systems was leached from basement rocks by upper crustal basinal fluid circulation driven by regional heat flow, likely due to lithospheric thinning and upwelling of the asthenosphere in the Late Mesozoic. The intracontinental hydrothermal systems and their continental sources with positive δ^{202}Hg and negative Δ^{199}Hg values are complementary to volcanic-arc and marine sedimentary rocks with opposite δ^{202}Hg - Δ^{199}Hg compositions. The distinct Hg isotopic features of hydrothermal systems in different tectonic settings, in particular the indelible Δ^{199}Hg signature, allow the tracing of large-scale material cycling in the Earth.

1. Introduction

Mercury is highly volatile and can be a potential tracer for temperature-sensitive processes during planet formation and evolution (Meier et al., 2016). Mercury has seven natural stable isotopes (196, 198-202, 204) which can undergo mass-dependent fractionation (MDF), usually defined as δ^{202}Hg, and mass-independent fractionation (MIF), usually defined as Δ^{199}Hg (Bergquist and Blum, 2007). The two-dimensional δ^{202}Hg-Δ^{199}Hg tracing scheme is particularly useful in understanding Hg sources in modern ecosystems, paleo-environmental change, early planetary evolution, and the origin of metals in ore deposits (Sherman et al., 2009; Blum et al., 2014; Meier et al., 2016; Grasby et al., 2020; Moynier et al., 2020; Shen et al., 2022). The framework of Hg isotope geochemistry (e.g., source signatures and isotope fractionation processes) in Earth's surface environment has been well established (Blum et al., 2014), given that Hg is a heavy metal pollutant of global concern. However, the isotopic geochemistry of Hg in Earth's interior reservoirs remains poorly constrained.

Mercury abundance varies greatly among geological reservoirs (Lauretta et al., 1999; Meier et al., 2016; Deng et al., 2021b). It is very low in igneous rocks (usually several ppb) (Meier et al., 2016), but can reach elevated levels (several ppm to several percent) in low-temperature (epithermal) hydrothermal systems (Zhu

* Corresponding author.
E-mail address: yinrunsheng@mail.gyig.ac.cn (R. Yin).

https://doi.org/10.1016/j.epsl.2022.117646
0012-821X/

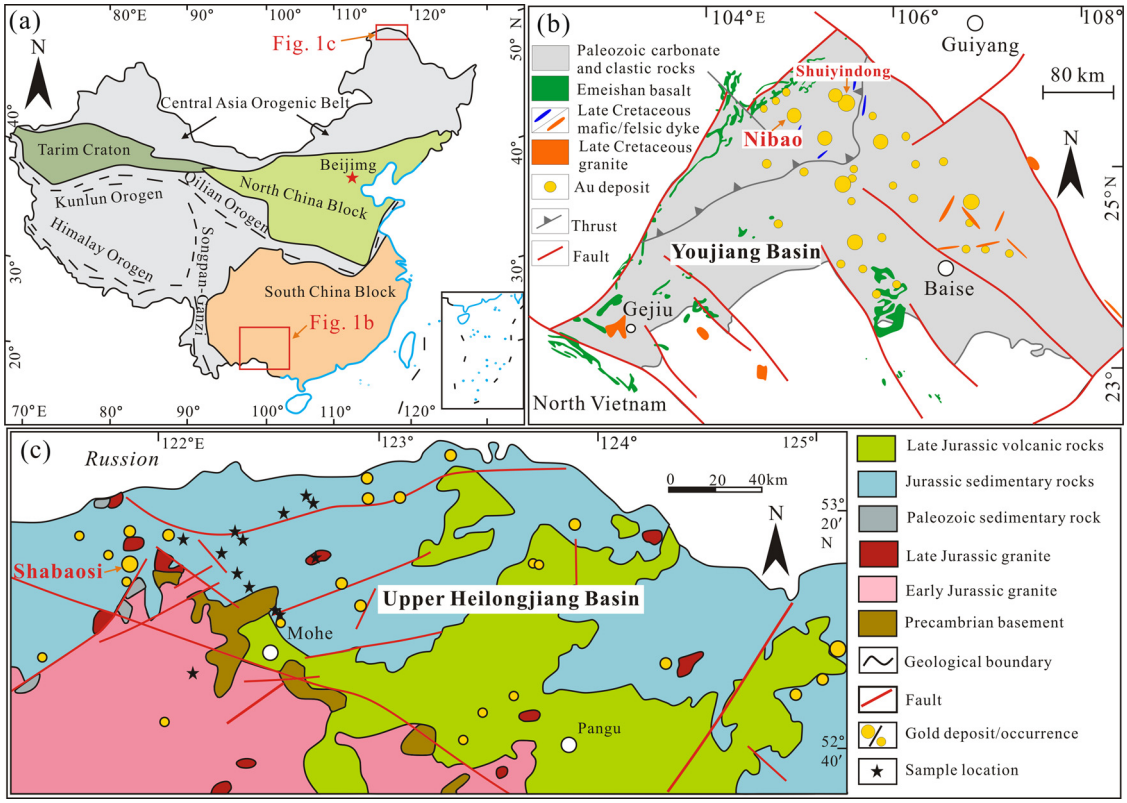

Fig. 1. (a) Simplified map of China showing major tectonic domains in China (after Zheng et al., 2013; Goldfarb et al., 2019). (b) Simplified geological map of the Youjiang Basin in South China showing the distribution of hydrothermal gold deposits (revised from Chen et al., 2011). (c) Geological sketch map showing the distribution of hydrothermal gold deposits in the Upper Heilongjiang Basin in North China (after Wu et al., 2006). (For interpretation of the colors in the figure(s), the reader is referred to the web version of this article.)

et al., 1986; Sherman et al., 2009; Deng et al., 2021a). Therefore, hydrothermal systems can record key information about Hg isotope heterogeneity, partitioning and transport in Earth's interior, and help to understand the global Hg cycle. Notably, a pioneer study on hydrothermal systems in Nevada, USA, reported an up to 5‰ variation of δ^{202}Hg, suggesting that hydrothermal processes can trigger significant Hg-MDF (Smith et al., 2005). Several subsequent studies then used δ^{202}Hg signals to illustrate fluid boiling and mineral precipitation (Sherman et al., 2009; Deng et al., 2021b).

Hg-MIF of the odd-mass isotopes (^{199}Hg, ^{201}Hg), commonly expressed as Δ^{199}Hg, is nearly exclusively produced by photochemical reactions in the atmosphere and at the surface of Earth (Bergquist and Blum, 2007), and therefore can be used as an indelible tracer of Hg recycling from surface reservoirs to the deep Earth (Deng et al., 2021a, 2021b; Moynier et al., 2021; Yin et al., 2022). This tracing is due to the distinctly negative Hg-MIF of terrestrial sub-aerially formed reservoirs, while oceanic reservoirs (marine sediments and seawater) have positive Hg-MIF (Blum et al., 2014; Shen et al., 2019, 2022). There is no Hg-MIF during hydrothermal processes (Yin et al., 2019; Fu et al., 2020), and Δ^{199}Hg values can also be used as a tracer of Hg recycling from surface reservoirs to hydrothermal systems (e.g., Cabral et al., 2022; Deng et al., 2022a).

To date, a comprehensive Hg dataset for hydrothermal systems in intracontinental settings is lacking, which limits our understanding of Hg cycling within the continental interior. Here, we present systematic research on two intracontinental hydrothermal systems in the Youjiang Basin of the South China craton and the Upper Heilongjiang Basin of the eastern Central Asian Orogenic Belt (CAOB), respectively, to characterize their Hg isotopic compositions. Potential source rocks for these systems (e.g., Precambrian basement, sedimentary rocks and volcanic arc granites) were also studied to understand the Hg source and migration processes. We observe uniform positive δ^{202}Hg and negative Δ^{199}Hg in both hydrothermal systems studied. Combined with the geotectonic background of these systems, we propose a deep fluid leaching model to explain the recycling of basement Hg into the intracontinental hydrothermal systems.

2. Geological background

2.1. Youjiang Basin

The Youjiang Basin is situated in the southwestern part of the Yangtze Block (Fig. 1A and 1B) and contains the greatest abundance of hydrothermal gold deposits (>800 tonnes Au) in the South China Craton (Hu et al., 2017). Hydrothermal systems in the Youjiang Basin are hosted in Paleozoic to Early Mesozoic platform carbonate and siliciclastic rocks and locally in Late Permian mafic intrusions or volcanic clastic rocks and show strong enrichment of As, Hg, Tl and Sb, besides Au (Goldfarb et al., 2019). Geochronological studies have shown that these systems were mainly formed during the Triassic (such as the giant Lannigou and the large Jinya Au deposits) and Late Jurassic-Early Cretaceous (such as the giant Shuiyindong, Nibao and Zimudang Au deposits, Hu et al., 2017). The ore mineralogy of these systems is dominated by pyrite, arsenopyrite, marcasite, stibnite, orpiment and realgar (Goldfarb et al., 2019).

The Hg isotopic data of the carbonate-hosted Shuiyindong deposit in the Youjiang Basin were previously reported by Yin et al. (2019). In order to identify if this Hg isotope pattern is of broader significance, we chose the Nibao deposit in southwestern Guizhou which is pyroclastic breccia-hosted. The 141 Ma Nibao Au deposit is situated along the northwestern margin of the Youjiang Basin

(Chen et al., 2019; Fig. 1B). The disseminated and vein-style mineralization is hosted in brecciated and silicified limestone, tuff and argillic rocks. Gold mainly occurs in zoned pyrite and arsenopyrite. Xie et al. (2016) indicated that the system formed under epithermal conditions of low salinity (8.2 wt% NaCl eq.) and low temperature (125 to 278 °C). Our microscope studies found that mercury exists mainly as solid solution in sulfides (e.g., pyrite, arsenopyrite, sphalerite, and realgar).

2.2. Upper Heilongjiang Basin

The E-W trending Upper Heilongjiang Basin is located in the northeastern part of the Central Asian Orogenic Belt (Fig. 1A and 1C). It is one of the most important Au provinces in China with dozens of newly discovered sandstone-hosted Au deposits. The Precambrian basement of the Upper Heilongjiang Basin is composed of the Xinghuadukou Group with rock associations of schist, gneiss, amphibolite, migmatite and marble (HBGMR, 1993; Hou et al., 2020), mainly exposed in the southern margin of the Upper Heilongjiang Basin (Fig. 1C). Scattered early Paleozoic strata consisting of schist, phyllite, slate and marbles were also identified in the western margin of the Upper Heilongjiang Basin (Liu et al., 2015). Outcrops within the Upper Heilongjiang Basin mainly consist of Middle Jurassic sandstones with scattered Late Jurassic granitoids. Large volumes of the Early Jurassic granites and Late Jurassic-Early Cretaceous volcanic cover are distributed in the southern margin of the Upper Heilongjiang Basin. Hydrothermal gold deposits in the Upper Heilongjiang Basin are mainly represented by Early Cretaceous moderate to low temperature hydrothermal systems with significant enrichment of Au, Hg, and Sb, such as the large Shabaosi and Baoxinggou Au deposits, which are hosted mainly in N-trending faults and brittle-ductile shear zones in Middle Jurassic clastic rocks (Fig. 1C; Wu et al., 2006; Li, 2015).

The large sandstone-hosted Shabaosi Au deposit is situated in the western part of the Upper Heilongjiang Basin (Fig. 1C). The ore bodies of the 130 Ma Shabaosi deposit are hosted in N-S trending altered fault zones in the Middle Jurassic sandstone and siltstone (Liu et al., 2015). The mineralization at Shabaosi occurs as quartz stockworks and disseminated sulfides in the sandstones. Sulfide minerals including pyrite, stibnite, galena, and sphalerite account for less than 1% of the bulk ore volume. Mercury is in solid solution in these sulfides. Fluid inclusion studies indicate that the ore-forming fluids belong to the H_2O-NaCl-CO_2-CH_4 system, with low salinity (0.8-8.3 wt% NaCl eq.) and low to moderate temperatures (180 to 320 °C) (Liu et al., 2015). Although the Shabaosi hydrothermal system is in the Central Asian Orogenic Belt, previous studies have shown that it formed in a post-subduction intracontinental setting, due to the closure of the adjacent Mongol-Okhotsk Ocean which ended during the Late Jurassic-Early Cretaceous (Wu et al., 2006; Deng et al., 2019).

3. Samples and analytical methods

Twenty-four mineralized quartz vein samples (five of them were prepared for pyrite concentrates) from the Nibao deposit and twenty quartz vein samples from the Shabaosi deposit were collected. In addition, eleven regionally distributed non-altered sandstones within the Upper Heilongjiang Basin, and two volcanic arc granites adjacent to the Upper Heilongjiang Basin were collected (for sample locations see Fig. 1C). The previously documented Hg isotopic data from the Precambrian basement and sedimentary rocks within or adjacent to the Upper Heilongjiang and Youjiang basins (Yin et al., 2017, 2019; Deng et al., 2022a, 2022b) are compiled here for comparison.

Total Hg (THg) concentrations of the samples were measured using a DMA-80 Hg analyzer with a Hg detection limit of 0.01 ng/g. Measurements of standard reference material (GSS-4, soil and GSR-2, andesite) showed recoveries of 95-100%. The coefficients of variation for triplicate analyses were <10%.

The samples were prepared for Hg isotope analysis following the double-stage thermal combustion and pre-concentration protocol (Zerkle et al., 2020). Standard reference material (GSS-4 and GSR-2) and method blanks were prepared in the same way as the samples to monitor the Hg recovery and lab contamination, respectively. The former yielded Hg recoveries of 95-100% and the latter show Hg concentrations lower than the detection limit, precluding laboratory contamination. The preconcentrated solutions were diluted to 1 ng/mL Hg and measured by a Neptune Plus multi-collector inductively-coupled plasma mass spectrometer (MC-ICP-MS), following the method by Yin et al. (2016). Hg-MDF is expressed in δ^{202}Hg notation in units of ‰ referenced to the NIST-3133 Hg standard (analyzed before and after each sample):

$$\delta^{202}\mathrm{Hg}(‰) = [(^{202}\mathrm{Hg}/^{198}\mathrm{Hg}_{\mathrm{sample}})/(^{202}\mathrm{Hg}/^{198}\mathrm{Hg}_{\mathrm{standard}}) - 1] \times 1000$$

MIF is reported in Δ notation, which describes the difference between the measured δ^{xxx}Hg and the theoretically predicted δ^{xxx}Hg value, in units of ‰:

$$\Delta^{xxx}\mathrm{Hg} = \delta^{xxx}\mathrm{Hg} - \delta^{202}\mathrm{Hg} \times \beta$$

β is 0.2520 for ^{199}Hg, 0.5024 for ^{200}Hg, and 0.7520 for ^{201}Hg (Blum and Bergquist, 2007). Analytical uncertainty was estimated based on the replication of the NIST-3177 standard solution. The overall average and uncertainty of NIST-3177 (δ^{202}Hg: −0.54 ± 0.10‰; Δ^{199}Hg: −0.02 ± 0.06‰; Δ^{201}Hg: −0.02 ± 0.08‰, 2SD, n = 18) and GSR-2 (δ^{202}Hg: −1.62 ± 0.14‰; Δ^{199}Hg: 0.05 ± 0.10‰; Δ^{201}Hg: 0.02 ± 0.08‰, 2SD, n = 4) agree well with previous studies (Blum and Bergquist, 2007; Geng et al., 2018). The 2SD of NIST-3177 with δ^{202}Hg, Δ^{199}Hg, and Δ^{201}Hg of 0.10‰, 0.06‰ and 0.08‰, respectively, represent the analytical uncertainties of our samples.

4. Results

Sample information, new data of Hg concentration and Hg isotopic composition of the investigated samples are presented in Supplementary Table 1. Specifically, pyrite samples from the Nibao deposit show the highest Hg concentrations (12.6 to 30.5 ppm). Quartz vein and pyritized wall rock samples from the Shabaosi and Nibao deposits show relatively lower Hg concentrations of 0.110 to 5.21 ppm and 0.208 to 7.64 ppm, respectively. The Jurassic sandstone and Mesozoic igneous rocks in the Upper Heilongjiang Basin show Hg contents of 1.00 to 35.0 ppb and 1.00 to 26.0 ppb, respectively.

As shown in Fig. 2, samples from the Shabaosi and Nibao deposits show δ^{202}Hg values of −0.25 to 1.35‰ and 0.48 to 1.41‰, respectively, and similar Δ^{199}Hg values of −0.22 to −0.02‰ and −0.24 to −0.05‰, respectively. The Mesozoic granites have δ^{202}Hg values of −3.76 to −3.11‰ and Δ^{199}Hg values of 0.07 to 0.18‰. The Jurassic sandstone samples have δ^{202}Hg values of −2.19 to 0.08‰ and Δ^{199}Hg values of −0.08 to 0.11‰.

5. Discussion

5.1. Continental origin for Hg in intracontinental hydrothermal systems

Previous studies have shown a distinct difference in Δ^{199}Hg in Earth's surface reservoirs, with globally positive Δ^{199}Hg values in the marine system and negative Δ^{199}Hg values in the continental system (Blum et al., 2014 and references therein, Grasby et al.,

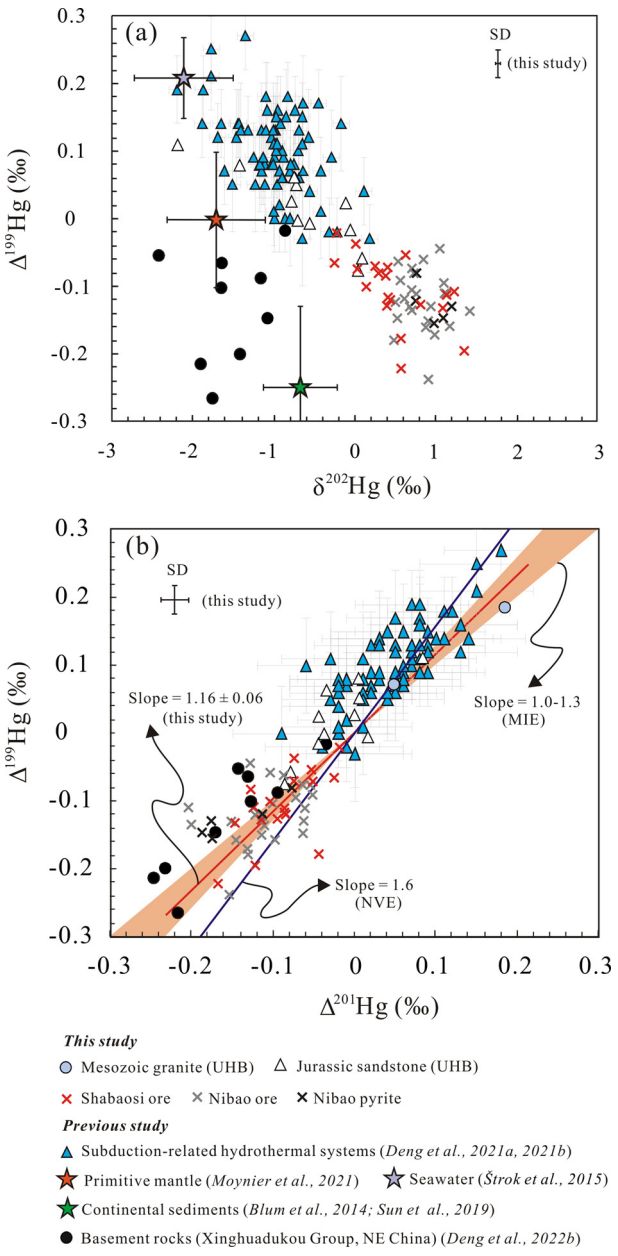

Fig. 2. (a) Δ^{199}Hg versus δ^{202}Hg diagram and (b) Δ^{199}Hg versus Δ^{201}Hg diagram for the samples studied. UHB-Upper Heilongjiang Basin. Data for the subduction-related hydrothermal systems in NE China are from Deng et al. (2021a, 2021b), for primitive mantle are from Moynier et al. (2021), for seawater are from Štrok et al. (2015) and for continental sediments are from Blum et al. (2014) and Sun et al. (2019).

2020; Shen et al., 2020, 2022). In comparison, primitive mantle rocks have Δ^{199}Hg values close to ~0‰ (Sherman et al., 2009; Moynier et al., 2021). The negative Δ^{199}Hg values in the ore samples from the Nibao and Shabaosi Au deposits are different from those in the primitive mantle. They are also different from previous results on subduction-related epithermal gold deposits in NE China and elsewhere, which have positive Δ^{199}Hg values due to the recycling of Hg from marine systems into these hydrothermal systems (Fig. 3; Deng et al., 2021a). Therefore, the source of Hg in the two intracontinental hydrothermal systems studied is likely not related to a subducting slab or (slab-fluid metasomatized) mantle. Marine sedimentary rocks in South China, such as Cambrian black shales and Triassic limestones, can be excluded as the Hg source for the Nibao deposit, due to their positive Δ^{199}Hg values (Fig. 3; Yin et al., 2017, 2019). The ore samples from the Shabaosi Au deposit with similar Δ^{199}Hg values are also distinctly with respect to their Δ^{199}Hg values to the nearby volcanic arc granites and the regionally distributed non-altered Jurassic sandstones (Fig. 3), precluding juvenile lower crustal melt and wall rocks, respectively, as Hg sources.

The negative Δ^{199}Hg values in the two deposits studied are similar to previous results on terrestrial reservoirs (e.g., soil and vegetation), characterized by negative Δ^{199}Hg signals (Blum et al., 2014 and reference therein), implying a terrestrial source of Hg. Considering that the ore samples from the Au deposits studied all have negative Δ^{199}Hg similar to the upper crustal Precambrian basement rocks adjacent and below the basins (Fig. 3), we infer that Hg in the hydrothermal systems studied from both the Youjiang and Upper Heilongjiang Basins is derived from these basement rocks. A similar situation applies to the Xikuangshan Sb deposit in the Xiangzhong Basin on the Yangtze block which also has negative Δ^{199}Hg values and for which a supracrustal basement Hg source was proposed (Fu et al., 2020) (Fig. 3). The very similar negative Δ^{199}Hg values for the Nibao and Shuiyindong Au deposits, as well as for the Xikuangshan Sb deposit (Yin et al., 2019; Fu et al., 2020), correspond to those observed for upper crustal basement rocks and strongly suggest a common basement Hg source for these deposits, and possibly the low-temperature deposits in South China in general.

Hg-MIF can be explained by either the magnetic isotope effect (MIE) or the nuclear volume effect (NVE). The MIE is induced by the photoreduction of Hg(II) or aqueous methylmercury (MeHg) photodegradation (Bergquist and Blum, 2007), whereas the NVE is caused during Hg(II)-thiol complexation, Hg(0) evaporation and Hg(II) reduction in the absence of light (Wiederhold et al., 2010; Zheng and Hintelmann, 2010; Ghosh et al., 2013). Both processes imprint specific Δ^{199}Hg/Δ^{201}Hg ratios. The MIE shows Δ^{199}Hg/Δ^{201}Hg ratios of 1.0 to 1.3, whereas the NVE produces Δ^{199}Hg/Δ^{201}Hg ratios of 1.60 to 1.65 (Bergquist and Blum, 2007; Zheng and Hintelmann, 2010; Blum et al., 2014). All samples in this study have a Δ^{199}Hg/Δ^{201}Hg ratio of 1.16 ± 0.06 (Fig. 2b), consistent with that observed during aqueous Hg(II) photoreduction (Bergquist and Blum, 2007) and typical of Earth's surface samples in general (e.g., soil, sediment, vegetation, seawater; Blum et al., 2014). Therefore, the observed Hg-MIF in our samples is a strong indication of the recycling of Hg from subaerial surface reservoirs into the hydrothermal systems. The upper crustal basement strata in the Youjiang (Lengjiaxi and Banxi Groups) and Upper Heilongjiang basins (Xinghuadukou Group) were formed in coastal settings (HBGMR, 1993; Zhao and Cawood, 2012), which receive large amounts of Hg through continental erosion which results in negative Δ^{199}Hg values in coastal sedimentary rocks (Yin et al., 2015). As metamorphism does not affect the primary Hg-MIF signature, it is believed that the metamorphic basement rocks reflect the Δ^{199}Hg values of their sedimentary protoliths (Deng et al., 2022b).

5.2. Significant geological reservoirs with isotopically heavy Hg

Previous studies documented mainly negative δ^{202}Hg values in geological reservoirs such as ordinary chondrites (−3.3 ± 0.9‰, 1SD; Meier et al., 2016; Moynier et al., 2020) and global basalts (−1.9 ± 0.6‰, 1SD; Geng et al., 2018; Moynier et al., 2021; Yin et al., 2022), crustal soil and sediments (−0.7 ± 0.5‰, 1SD; Blum et al., 2014 and references therein), and subduction-related epithermal deposits in NE China and the Pacific Rim (−0.75 ± 0.93‰, n = 182, 1SD; Deng et al., 2021a, 2021b and references therein). These results are quite different from the positive δ^{202}Hg values observed in samples from the intracontinental hydrothermal systems in the Youjiang, Upper Heilongjiang and Xiangzhong

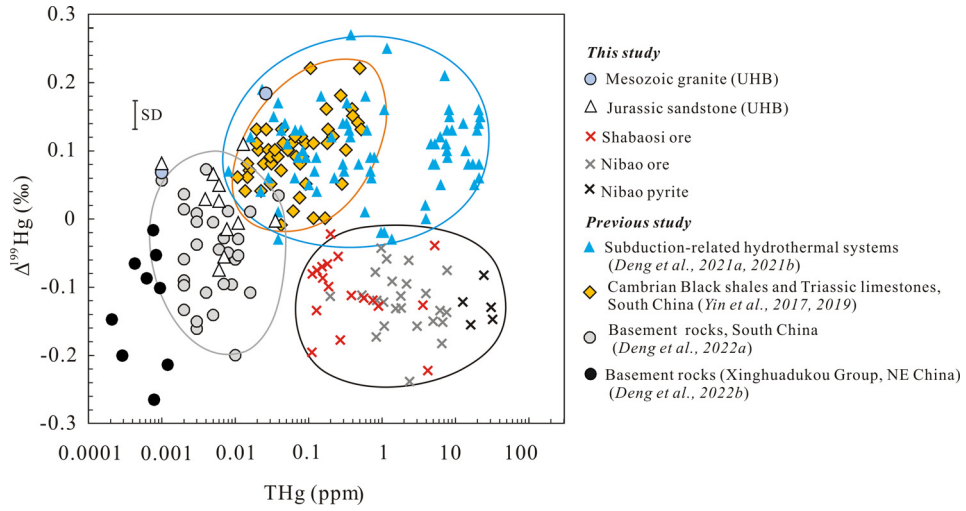

Fig. 3. Plot of Δ^{199}Hg vs. Hg concentration of samples from the Youjiang and Upper Heilongjiang basins. UHB-Upper Heilongjiang Basin. Subduction-related hydrothermal systems in NE China (Deng et al., 2021a, 2021b) are defined in the area with a blue line boundary, intracontinental hydrothermal systems (this study) are defined in the area with a black line boundary, Cambrian black shales and Triassic limestones in South China (Yin et al., 2017, 2019) are defined in the area with an orange line boundary, and basement rocks in South China (Deng et al., 2022a) in the area with a gray line boundary.

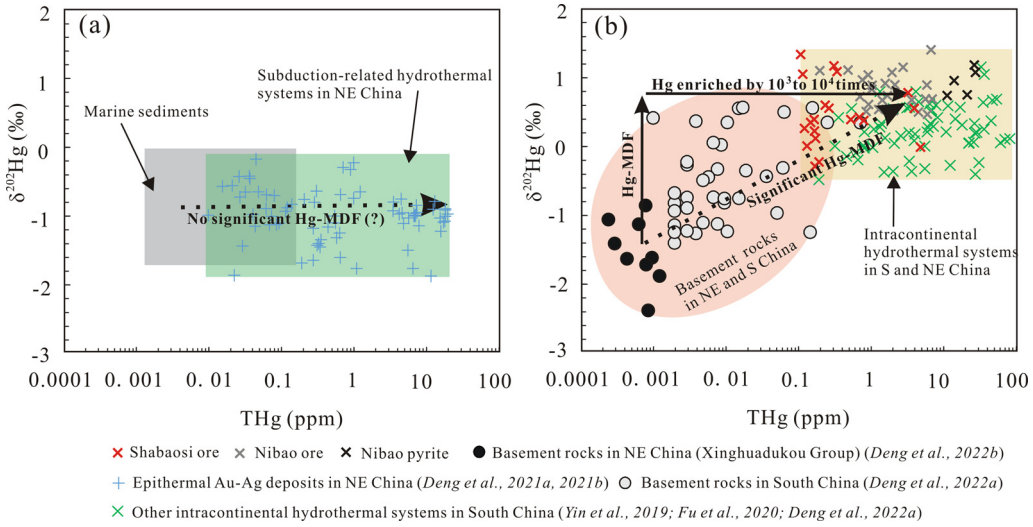

Fig. 4. (A) Plot of δ^{202}Hg vs. Hg concentration of samples from marine sedimentary rocks and subduction-related hydrothermal systems. Data for the subduction-related hydrothermal systems in NE China are from Deng et al. (2021a, 2021b). (B) Plot of δ^{202}Hg vs. THg of samples in this study and from Yin et al. (2019), Fu et al. (2020) and Deng et al. (2022a).

basins (Fig. 3), which show an average δ^{202}Hg value of 0.49 ± 0.46‰ (1SD, n = 129) and demonstrate a significant enrichment of isotopically heavy Hg in the intracontinental hydrothermal systems.

In the δ^{202}Hg vs. Δ^{199}Hg diagram (Fig. 2a), the hydrothermal deposits of the Youjiang and Upper Heilongjiang basins are separated from the subduction-related deposits in NE China, which implies a different geochemical behavior of Hg between the two systems. Mercury in the subduction-related epithermal systems is interpreted to be released from subducted marine sediments (Deng et al., 2021a, 2021b), and then transported by hydrothermal fluids. As shown in Fig. 4a, subduction-related epithermal systems have δ^{202}Hg values similar to marine sediments, suggesting small or no Hg-MDF in the formation of subduction-related magmatic-hydrothermal systems. It is likely that under high-temperature conditions, due to the high volatility of Hg, most of the Hg from the oceanic slab would be released and enter the hydrothermal fluids, triggering limited Hg-MDF. In contrast, the intracontinental hydrothermal systems generally show Hg-MDF signals distinctly different from their basement source (Fig. 4b), indicating that significant Hg-MDF can occur during the formation of these systems. The positive δ^{202}Hg values in the hydrothermal deposits in both Youjiang and Upper Heilongjiang basins were possibly caused by the preferential leaching of isotopically heavier Hg from the basement rocks by basinal fluids, as experimental studies on the leaching of Hg from sedimentary materials demonstrate the enrichment of heavier Hg isotopes in the leachates (Stetson et al., 2009). Overall, we suggest that Hg in arc-related and intracontinental hydrothermal systems may have experienced different patterns of Hg-MDF. Given that the formation of hydrothermal systems involves various processes (Hu et al., 2017; Goldfarb et al., 2019), the reason for the δ^{202}Hg difference between these two distinct hydrothermal settings likely not only depends on temperature. Future experimental work may improve our understanding of the enrichment of isotopically heavy Hg in intracontinental hydrothermal systems.

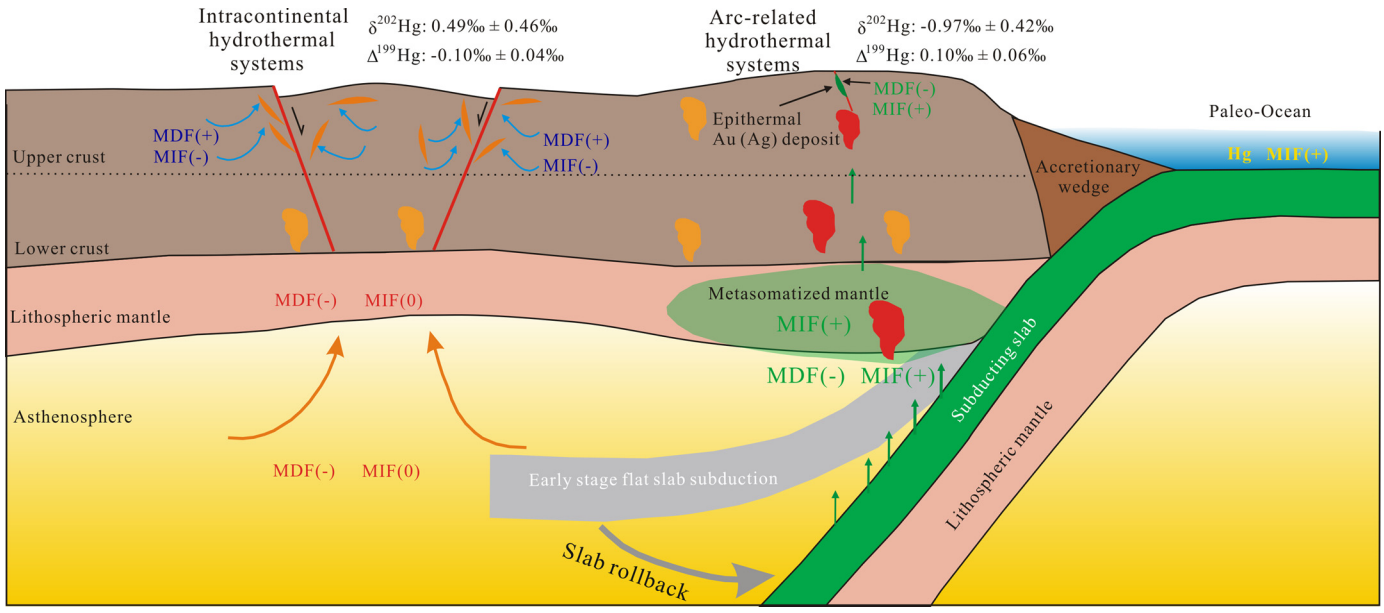

Fig. 5. Genetic model showing the formation of the late Mesozoic intracontinental hydrothermal systems in the Upper Heilongjiang and Youjiang basins, China. Intracontinental Hg cycling at extensional settings leads to specific Hg isotopic reservoirs with δ^{202}Hg values of 0.49 ± 0.46‰, and Δ^{199}Hg values of −0.10 ± 0.04‰, which are distinctly different to the primitive mantle (δ^{202}Hg: −1.7 ± 0.6‰, Δ^{199}Hg: 0.00 ± 0.10‰; Moynier et al., 2021) and subduction-related hydrothermal systems (δ^{202}Hg: −0.97 ± 0.42‰, Δ^{199}Hg: 0.10 ± 0.06‰; Deng et al., 2021a, 2021b).

5.3. Recycling of Hg in the intracontinental setting

Hydrothermal systems in continental arc settings commonly show positive Δ^{199}Hg values (Blum et al., 2014; Deng et al., 2021b), due to the contribution of recycled Hg from the subducting oceanic slab (Fig. 5; Deng et al., 2021a). Based on the negative Δ^{199}Hg values in our samples and the geotectonic backgrounds of the Youjiang and Upper Heilongjiang basins, below we propose an upper crustal fluid recycling of continental Hg into the intracontinental hydrothermal systems.

Both South China and NE China experienced a period of flat subduction of the Paleo-Pacific oceanic slab during the Jurassic and slab foundering and rollback during the Late Jurassic-Early Cretaceous (Li and Li, 2007; Kiminami and Imaoka, 2013). Geochronological studies by Liu et al. (2015) and Chen et al. (2019) show that the formation of the Late Mesozoic gold deposits in both Youjiang and Upper Heilongjiang basins is coincident with the foundering and rollback of the flat slab. The studied hydrothermal systems formed in an extensional intracontinental setting, which is different from the epithermal hydrothermal systems in subduction-controlled volcanic arcs (Hu et al., 2017; Goldfarb et al., 2019). In intracontinental settings such as back-arc basins, long-term sub-aerial sedimentation of continental materials (e.g., soil and plants), can accumulate massive amounts of atmospheric Hg(0) with negative δ^{202}Hg and Δ^{199}Hg. These terrestrial materials underwent subsequent diagenesis and metamorphism to form the basement with negative Δ^{199}Hg values. During large-scale extensional events, the thermal flow caused by lithospheric thinning and asthenospheric upwelling can drive the circulation of upper crustal basinal brines which leach metals, including Hg. Likely, the intracontinental hydrothermal systems in the Youjiang and Upper Heilongjiang basins were driven by elevated heat flow from the rise of the asthenosphere as compensation for the foundering slab (Li and Li, 2007) (Fig. 5). More importantly, the negative Δ^{199}Hg values in our samples identify intracontinental hydrothermal deposits and their supracrustal basement rocks as an unrecognized isotopically light Hg pool, distinguished from the primitive mantle with near-zero Δ^{199}Hg values and complementary to the arc-related hydrothermal systems with positive Δ^{199}Hg values.

6. Conclusions and implications

This study demonstrates that hydrothermal systems formed in different tectonic settings can have distinct Hg isotopic compositions due to their distinct Hg sources and Hg mobilization pathways. Arc-related hydrothermal systems formed in convergent continental margins are mainly characterized by negative δ^{202}Hg (−0.97 ± 0.42‰, 1SD, n = 73) and positive Δ^{199}Hg (0.10 ± 0.06‰, 1SD, n = 73) values (Deng et al., 2021a, 2021b), due to the recycling of Hg from subducted marine sediments into these deposits. Intracontinental hydrothermal systems formed far from subduction zones can have positive δ^{202}Hg values (0.49 ± 0.46‰, 1SD, n = 129) and negative Δ^{199}Hg (−0.10 ± 0.04‰, 1SD, n = 129) values, due to remobilization and of metals (including Hg) from basement rocks. Notably, the large variability of Δ^{199}Hg in these two distinct settings of hydrothermal systems, different from the near-zero Δ^{199}Hg values in the primitive mantle (Moynier et al., 2021), indicates that a significant fraction of Hg has undergone Hg(II) photoreduction on Earth's surface, prior to lithospheric recycling. Our study provides new insights into the global cycling of Hg in the crustal environment. In particular, the opposing Δ^{199}Hg values in arc-related and intracontinental hydrothermal systems illustrate that Hg was recycled from marine reservoirs through plate subduction and from continental reservoirs by intracontinental fluid circulation, respectively.

CRediT authorship contribution statement

Changzhou Deng: Investigation, Writing – original draft. **Bernd Lehmann:** Conceptualization, Investigation, Writing – original draft. **Tingting Xiao:** Data curation, Investigation. **Qinping Tan:** Data curation, Investigation. **Di Chen:** Data curation, Investigation. **Zhendong Tian:** Data curation, Investigation. **Xueyun Wang:** Data curation, Investigation. **Guangyi Sun:** Data curation, Investigation.

Runsheng Yin: Conceptualization, Methodology, Supervision, Writing – original draft.

Declaration of competing interest

The authors declare that they have no known competing financial interests or personal relationships that could have appeared to influence the work reported in this paper.

Acknowledgements

This work was supported by the National Natural Science Foundation of China (41873047). We especially thank Jishuang Ding and Sheng Lu for help with field sampling.

Appendix A. Supplementary material

Supplementary material related to this article can be found online at https://doi.org/10.1016/j.epsl.2022.117646.

References

Bergquist, B.A., Blum, J.D., 2007. Mass-dependent and -independent fractionation of Hg isotopes by photoreduction in aquatic systems. Science 318, 417–420.
Blum, J.D., Bergquist, B.A., 2007. Reporting of variations in the natural isotopic composition of mercury. Anal. Bioanal. Chem. 388, 353–359.
Blum, J.D., Sherman, L.S., Johnson, M.W., 2014. Mercury isotopes in Earth and environmental sciences. Annu. Rev. Earth Planet. Sci. 42, 249–269.
Cabral, A.R., Deng, C.Z., Yin, R.S., Yakubovich, O.V., Stuart, F.M., Tupinamba, M., Lehmann, B., 2022. Metal recycling tracked by mercury and helium isotopes in platinum-palladium nuggets from Corrego Bom Sucesso, Brazil. Chem. Geol. 593, 120752.
Chen, M.H., Mao, J.W., Bierlein, F.P., Norman, T., Uttley, P.J., 2011. Structural features and metallogenesis of the Carlin-type Jinfeng (Lannigou) gold deposit, Guizhou Province, China. Ore Geol. Rev. 43, 217–234.
Chen, M.H., Bagas, L., Liao, X., Zhang, Z.Q., Li, Q.L., 2019. Hydrothermal apatite SIMS Th-Pb dating: constraints on the timing of low-temperature hydrothermal Au deposits in Nibao, SW China. Lithos 324–325, 418–428.
Deng, C.Z., Sun, D.Y., Han, J.S., Chen, H.Y., Li, G.H., Xiao, B., Li, R.C., Feng, Y.Z., Li, C.L., Lu, S., 2019. Late-stage southwards subduction of the Mongol-Okhotsk oceanic slab and implications for porphyry Cu-Mo mineralization: constraints from igneous rocks associated with the Fukeshan deposit, NE China. Lithos 326–327, 341–357.
Deng, C.Z., Sun, G.Y., Rong, Y.M., Sun, R.Y., Sun, D.Y., Lehmann, B., Yin, R.S., 2021a. Recycling of mercury from the atmosphere-ocean system into volcanic-arc-associated epithermal gold systems. Geology 49, 309–313.
Deng, C.Z., Li, C.L., Rong, Y.M., Chen, D., Zhou, T., Wang, X.Y., Chen, H.Y., Lehmann, B., Yin, R.S., 2021b. Different metal sources in the evolution of an epithermal ore system: evidence from mercury isotopes associated with the Erdaokan epithermal Ag-Pb-Zn deposit, NE China. Gondwana Res. 95, 1–9.
Deng, C.Z., Zhang, J.W., Hu, R.Z., Luo, K., Zhu, Y.N., Yin, R.S., 2022a. Mercury isotope constraints on the genesis of Late Mesozoic Sb deposits in South China. Sci. China Earth Sci. 65 (2), 269–281.
Deng, C.Z., Geng, H.Y., Xiao, T.T., Chen, D., Sun, G.Y., Yin, R.S., 2022b. Mercury isotopic compositions of the Precambrian rocks and implications for tracing mercury cycling in Earth's interior. Precambrian Res. 373, 106646.
Fu, S.L., Hu, R.Z., Yin, R.S., Yan, J., Mi, X.F., Song, Z.C., Sullivan, N.A., 2020. Mercury and in situ sulfur isotopes as constraints on the metal and sulfur sources for the world's largest Sb deposit at Xikuangshan, Southern China. Miner. Depos. 55, 1353–1364.
Geng, H.Y., Yin, R.S., Li, X.D., 2018. An optimized protocol for high precision measurement of Hg isotopic compositions in samples with low concentrations of Hg using MC-ICP-MS. J. Anal. At. Spectrom. 3, 1932–1940.
Ghosh, S., Schauble, E.A., Lacrampe Couloume, G., Blum, J.D., Bergquist, B.A., 2013. Estimation of nuclear volume dependent fractionation of mercury isotopes in equilibrium liquid-vapor evaporation experiments. Chem. Geol. 336, 5–12.
Goldfarb, R.J., Qiu, K.F., Deng, J., Chen, Y.J., Yang, L.Q., 2019. Orogenic gold deposits of China. In: Goldfarb, R.J., Chang, Z.S. (Eds.), Mineral Deposits of China. In: Society of Economic Geologists Special Publications, vol. 22, pp. 263–324.
Grasby, S.E., Liu, X.J., Yin, R.S., Richard, E.E., Chen, Z.H., 2020. Toxic mercury pulses into late Permian terrestrial and marine environments. Geology 48, 830–833.
HBGMR (Heilongjiang Bureau of Geology and Mineral Resources), 1993. Regional Geology of Heilongjiang Province. Geological Publishing House, Beijing (in Chinese with English abstract).
Hou, W.Z., Zhao, G.C., Han, Y.G., Eizenhoefer, P.R., Zhang, X.R., Liu, Q., 2020. A ~2.5 Ga magmatic arc in NE China: new geochronological and geochemical evidence from the Xinghuadukou Complex. Geol. J. 55, 2550–2571.
Hu, R.Z., Fu, S.L., Huang, Y., Zhou, M.F., Fu, S.H., Zhao, C.H., Wang, Y.J., Bi, X.W., Xiao, J.F., 2017. The giant South China Mesozoic low-temperature metallogenic domain: reviews and a new geodynamic model. J. Asian Earth Sci. 137, 9–34.
Kiminami, K., Imaoka, T., 2013. Spatiotemporal variations of Jurassic-Cretaceous magmatism in eastern Asia (Tan-Lu Fault to SW Japan): evidence for flat-slab subduction and slab rollback. Terra Nova 25, 414–422.
Lauretta, D.S., Devouard, B., Buseck, P.R., 1999. The cosmochemical behavior of mercury. Earth Planet. Sci. Lett. 171, 35–47.
Li, X.W., 2015. Metallogenic regularities of gold deposits in upper Heilongjiang metallogenic belt and its prospecting. Ph.D. thesis. Jilin University, Changchun, China (in Chinese with English abstract).
Li, Z.X., Li, X.H., 2007. Formation of the 1300-km-wide intracontinental orogen and postorogenic magmatic province in Mesozoic South China: a flat-slab subduction model. Geology 35, 179–182.
Liu, J., Wu, G., Qiu, H.N., Li, Y., 2015. $^{40}Ar/^{39}Ar$ dating, fluid inclusions and S-Pb isotope systematics of the Shabaosi gold deposit, Heilongjiang Province, China. Geol. J. 50, 592–606.
Meier, M.M.M., Cloquet, C., Marty, B., 2016. Mercury (Hg) in meteorites: variations in abundance, thermal release profile, mass-dependent and mass-independent isotopic fractionation. Geochim. Cosmochim. Acta 182, 55–72.
Moynier, F., Chen, J.B., Zhang, K., Cai, H.M., Wang, Z.C., Jackson, M.G., Day, J.M.D., 2020. Chondritic mercury isotopic composition of Earth and evidence for evaporative equilibrium degassing during the formation of eucrites. Earth Planet. Sci. Lett. 551, 116544.
Moynier, F., Jackson, M., Zhang, K., Cai, H., Halldórsson, S.A., Pik, R., Day, J.M.D., Chen, J., 2021. The mercury isotopic composition of Earth's mantle and the use of mass independently fractionated Hg to test for recycled crust. Geophys. Res. Lett. 48, e2021GL094301.
Shen, J., Algeo, T.J., Chen, J.B., Planavsky, N.J., Feng, Q.L., Yu, J.X., Liu, J.L., 2019. Mercury in marine Ordovician/Silurian boundary sections of South China is sulfide-hosted and non-volcanic in origin. Earth Planet. Sci. Lett. 511, 130–140.
Shen, J., Feng, Q., Algeo, T.J., Liu, J., Zhou, C., Wei, W., Liu, J., Them, T.R., Gill, B.C., Chen, J., 2020. Sedimentary host phases of mercury (Hg) and implications for use of Hg as a volcanic proxy. Earth Planet. Sci. Lett. 543, 116333.
Shen, J., Yin, R.S., Zhang, S., Algeo, T.J., Bottier, D.J., Yu, J.X., Xu, G.Z., Penman, D., Wang, Y.D., Li, L.Q., Shi, X., Planavsky, N.J., Feng, Q.L., Xie, S.C., 2022. Intensified continental chemical weathering and carbon-cycle perturbations linked to volcanism during the Triassic-Jurassic transition. Nat. Commun. 13, 299.
Sherman, L.S., Blum, J.D., Nordstrom, D.K., McCleskey, R.B., Barkay, T., Vetriani, C., 2009. Mercury isotopic composition of hydrothermal systems in the Yellowstone Plateau volcanic field and Guaymas Basin sea-floor rift. Earth Planet. Sci. Lett. 279, 86–96.
Smith, C.N., Kesler, S.E., Klaue, B., Blum, J.D., 2005. Mercury isotope fractionation in fossil hydrothermal systems. Geology 33, 825–828.
Stetson, S.J., Gray, J.E., Wanty, R.B., Macalady, D.L., 2009. Isotopic variability of mercury in ore, mine-waste calcine, and leachates of mine-waste calcine from areas mined for mercury. Environ. Sci. Technol. 43, 7331–7336.
Štrok, M., Baya, P.A., Hintelmann, H., 2015. The mercury isotope composition of Arctic coastal seawater. C. R. Geosci. 347, 368–376.
Sun, R.Y., Jiskra, M., Amos, H.M., Zhang, Y.X., Sunderland, E.M., Sonke, J.E., 2019. Modelling the mercury stable isotope distribution of Earth surface reservoirs: implications for global Hg cycling. Geochim. Cosmochim. Acta 246, 156–173.
Wiederhold, J.G., Daniel, K., Infante, I., et al., 2010. Equilibrium mercury isotope fractionation between dissolved Hg(II) species and thiol-bound Hg. Environ. Sci. Technol. 44, 4191–4197.
Wu, G., Sun, F.Y., Zhu, Q., Li, Z.T., Ding, Q.F., Li, G.Y., Pang, Q.B., Wang, H.B., 2006. Geological characteristics and genesis of gold deposits in Upper Heilongjiang Basin. Miner. Depos. 25, 215–230 (in Chinese with English abstract).
Xie, X.Y., Feng, D.S., Chen, M.H., Guo, S.X., Kuang, S.D., Chen, H.S., 2016. Fluid inclusion and stable isotope geochemistry study of the Nibao gold deposit, Guizhou and insight into ore genesis. Acta Petrol. Sin. 32, 3360–3376 (in Chinese with English abstract).
Yin, R., Feng, X., Chen, B., Zhang, J., Wang, W., Li, X., 2015. Identifying the sources and processes of mercury in subtropical estuarine and ocean sediments using Hg isotopic composition. Environ. Sci. Technol. 49, 1347–1355.
Yin, R., Krabbenhoft, D.P., Bergquist, B.A., Zheng, W., Lepak, R.F., Hurley, J.P., 2016. Effects of mercury and thallium concentrations on high precision determination of mercury isotopic composition by Neptune Plus multiple collector inductively coupled plasma mass spectrometry. J. Anal. At. Spectrom. 31, 2060–2068.
Yin, R., Xu, L., Lehmann, B., Lepak, R.F., Hurley, J.P., Mao, J.W., Feng, X.B., Hu, R.Z., 2017. Anomalous mercury enrichment in Early Cambrian black shales of South China: mercury isotopes indicate a seawater source. Chem. Geol. 467, 159–167.
Yin, R., Deng, C., Lehmann, B., Sun, G.Y., Lepak, R.F., Hurley, J.P., Zhao, C.H., Xu, G.W., Tan, Q.P., Xie, G.Z., Hu, R.Z., 2019. Magmatic-hydrothermal origin of mercury in Carlin-style and epithermal gold deposits in China: evidence from mercury stable isotopes. ACS Earth Space Chem. 3, 1631–1639.

Yin, R., Chen, D., Pan, X., Deng, C., Chen, L., Song, X., Yu, S., Zhu, C., Wei, X., Xu, Y., Feng, X., Blum, J.D., Lehmann, B., 2022. Mantle Hg isotopic heterogeneity and evidence of oceanic Hg recycling into the mantle. Nat. Commun. 13, 948.

Zerkle, A.L., Yin, R., Chen, C., Li, X.D., Izon, G.J., Grasby, S.E., 2020. Anomalous fractionation of mercury isotopes in the Late Archean atmosphere. Nat. Commun. 11, 1709.

Zhao, G.C., Cawood, P.A., 2012. Precambrian geology of China. Gondwana Res. 222–223, 13–54.

Zheng, W., Hintelmann, H., 2010. Nuclear field shift effect in isotope fractionation of mercury during abiotic reduction in the absence of light. J. Phys. Chem. A 114 (12), 4238–4245.

Zheng, Y.F., Xiao, W.J., Zhao, G.C., 2013. Introduction to tectonics of China. Gondwana Res. 23, 1365–1377.

Zhu, B.Q., Zhang, J.M., Zhu, L.X., Zheng, Y.X., 1986. Mercury, arsenic, antimony, bismuth and boron as geochemical indicators for geothermal areas. J. Geochem. Explor. 25, 379–388.